

U–Pb zircon SHRIMP evidence for Cambrian volcanism in the Schistose Domain within the Galicia-Trás-os-Montes Zone (Variscan Orogen, NW Iberian Peninsula)

P. FARIAS^{1*} B. ORDOÑEZ-CASADO¹ A. MARCOS¹ A. RUBIO-ORDOÑEZ¹ C.M. FANNING²

¹Departamento de Geología de la Universidad de Oviedo

C/ Jesús Arias de Velasco, s/n, 33005 Oviedo, Spain. Farias E-mail: pfarias@geol.uniovi.es Ordoñez-Casado E-mail: bertapablomara@gmail.com Marcos E-mail: marcos@geol.uniovi.es Rubio-Ordóñez E-mail: arubio@geol.uniovi.es

²Research School of Earth Sciences, the Australian National University, Canberra, Australia

Fanning E-mail: mark.fanning@anu.edu.au

ABSTRACT

SHRIMP U–Pb zircon analyses have shown the complexity of dating volcanic rocks due to the presence of inner cores within zircon crystals. Using the cathodoluminescence studies assisting ion microprobe analyses allow us to conclude that: the two low-grade metavolcanic samples from the Schistose Domain of the Galicia-Trás-os-Montes Zone in the northeast limb of the Verín-Bragança synform (NW Spain and NE Portugal) yield ages of 488.7 ± 3.7 Ma and 499.8 ± 3.7 Ma (lowermost Ordovician–Upper Cambrian). The Schistose Domain had been traditionally considered as a parautochthonous tectonic unit, i.e. as the stratigraphic continuation of the autochthonous underlying rocks, only locally or moderately detached from them as a result of strong dragging forces from large allochthonous units above it. Current interpretation of the Schistose Domain suggests that this domain formed the outboard edge of the Iberian terrane. Important Arenig, felsic magmatism with similar geochemical signature to the volcanic bodies in the Schistose Domain of the Galicia-Trás-os-Montes Zone (GTMSD) series is present also in the adjacent Ollo de Sapo Domain of the Central Iberian Zone. This contemporary nature of magmatic events provides an additional argument to support the “Iberian” affinity of the Schistose Domain of the Galicia-Trás-os-Montes Zone. However, the Cambro–Ordovician facies are very different in the Schistose Domain with respect to the autochthonous unit, the Central–Iberian Zone, suggesting that the Schistose Domain must be considered as a major allochthonous unit with a displacement of over several tens of kilometers.

KEYWORDS Variscan. Galicia-Trás-os-Montes Zone. Schistose Domain. SHRIMP U–Pb.

INTRODUCTION

The Schistose Domain, also named Para-autochthonous Thrust Complex (Ribeiro *et al.*, 1990), forms the lowermost tectonic unit of the Galicia-Trás-os-Montes Zone (GTMZ) (Farias *et al.*, 1987), the most internal one of the Variscan Belt in the NW of the Iberian Peninsula. It is constituted by a metasedimentary sequence more than 4000m thick interpreted as the most external sediments of the continental margin of Gondwana (Farias *et al.*, 1987; Ribeiro *et al.*, 1990,

Martínez Catalán *et al.*, 1999; Marcos *et al.*, 2002; Arenas *et al.*, 2004b; Murphy *et al.*, 2008; Díez Fernández *et al.*, 2012). The extension, geometrical relationships and stratigraphic differences with the neighboring regions allows the Schistose Domain to be considered as a major allochthonous Variscan unit with a displacement of over several tens of kilometres (Ribeiro, 1974; Farias *et al.*, 1987; Barrera *et al.*, 1989; Farias, 1990).

The age of the Schistose Domain is a subject of controversy. For a long time, these rocks were considered

Silurian in age either non-concordant with the Lower Palaeozoic series of de Central-Iberian Zone (ZCI) (Ferragne, 1972; Fernández Pompa and Monteserín López, 1976) or concordant and forming the upper part of the same series (Matte, 1968; Romariz, 1969; Iglesias and Robardet, 1980; Bastida *et al.*, 1984). However, all the recognized Silurian faunas (Graptolites) occur right below the Schistose Domain basal thrust (González Clavijo, 1997; Marcos and Farias, 1999; Marcos *et al.*, 2002; Marcos and Llana-Fúnez, 2002) in rocks that forms part of the autochthonous unit, represented by the Palaeozoic sequence of the Olla de Sapo antiform (Central-Iberian Zone, Fig. 1). Palaeontological findings in the Trás-Os-Montes (Pereira *et al.*, 2000) and Cabo Ortegal areas (Rodríguez *et al.*, 2004), as well as U-Pb dating of felsic volcanic rocks near the Cabo Ortegal Complex (Valverde-Vaquero *et al.*, 2005) and in the Verín synform (Valverde-Vaquero *et al.*, 2007), establish an Ordovician and Silurian age for some of the rocks of this domain. Furthermore, according to U-Pb detrital zircon analysis of this sequence the maximum sedimentation age is latest Neoproterozoic (c. 560Ma) (Díez Fernández *et al.*, 2012). In spite of this data, some authors (Piçarra *et al.*, 2006) still consider the Schistose Domain to be

Silurian in age, defending its “parautochthonous” character.

In this contribution we present U-Pb zircon-ages for rhyolitic and dacitic meta-volcanites interbedded in the lower part of the parautochthonous series in the Northeast limb of the Verín-Bragança-Alcañices synform. The cathodoluminescence (CL) studies on multiphase rocks show (*e.g.* Ordóñez-Casado, 1999, Ordóñez-Casado *et al.*, 2001) that the internal structure of zircons is frequently independent of its morphology. The microanalysis of the different domains within one zircon by means of Sensitive High Resolution Ion MicroProbe (SHRIMP) is considered among the most trustworthy methods to obtain radiometric data of magmatic and high-grade metamorphic rocks. This method allows us to avoid the inherited component of the inner cores, obtaining more reliable ages.

GEOLOGICAL SETTING

The GTMZ is the most internal zone of the Variscan Belt in the NW of the Iberian Peninsula (Fig. 1). It is thrustured over Palaeozoic rocks of the neighbouring

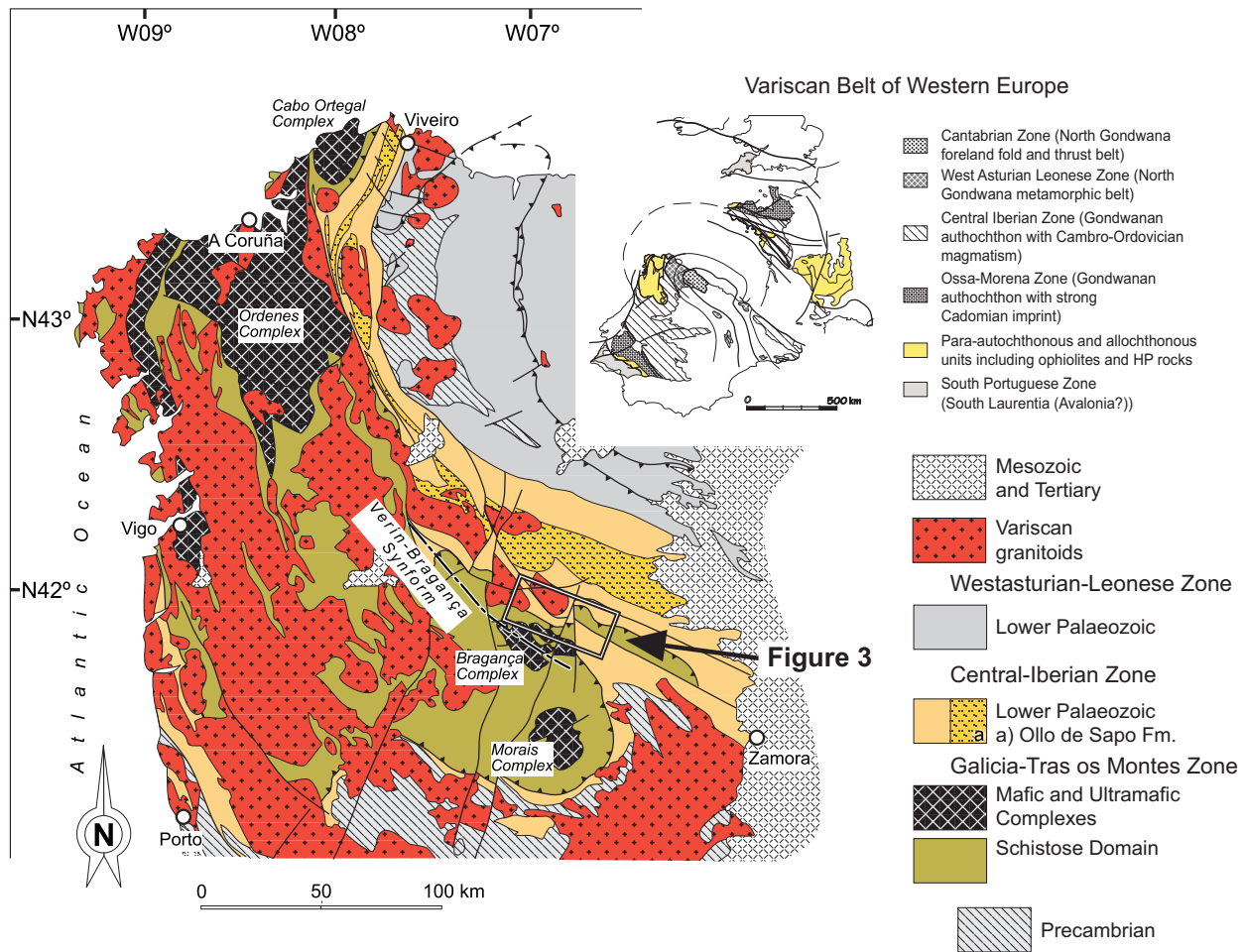


FIGURE 1. Geological sketch of the NW Iberian Peninsula, showing zones established by Lotze (1945), Julivert *et al.* (1972) and Farias *et al.* (1987).

CIZ. Two domains have been distinguished within the GTMZ: i) the Schistose Domain, composed by more than 4000m thick metasedimentary sequence with interbedded metavolcanics; and ii) the Allochthonous Complexes, tectonically emplaced over the former and composed by mafic–ultramafic and quartz–feldspathic rocks with different origin, grouped into different tectonic units (*e.g.* oceanic, ophiolitic and continental) (Farias *et al.*, 1987; see Arenas *et al.*, 2004a and references therein).

The Schistose Domain forms a thin sheet thrustured between the Bragança Allochthonous Complex and the underlying Lower Palaeozoic metasediments of the Olo de Sapo antiform (Farias, 1990; González Clavijo, 1997; González Clavijo and Martínez Catalán, 2002). Two stratigraphic units, the Nogueira and Paraño groups, have been established in the Schistose Domain. The former is mainly composed by black shales, lidites and scarce tobaceous–cineritic volcanites, with a minimum thickness of 500m. The Paraño Group constitutes a more than 3000m thick succession of siliciclastic rocks (phyllites, psamites, greywackes, quartzites and microconglomerates) with interbedded layers of metavolcanites, mainly rhyolites and some felsic trachytes (Fig. 2).

The rocks of the Schistose Domain have been deformed under greenschist facies conditions and affected by three main Variscan deformation episodes. They show a pervasive S1 cleavage related with tight folds that are visible only when affecting the quartzite beds. S2 phyllonite fabrics developed in association to the Galicia-Trás-os-Montes basal thrust and open right D3 folds at all scales, including crenulation cleavage, are folding the previous structures (Farias, 1990; Dallmeyer *et al.*, 1997; Marcos and Farias, 1999).

SAMPLE DESCRIPTION

Two samples (COS-7 and COS-8) were collected in metavolcanic levels outcropping close to the Spanish–Portuguese border in the Bragança–Alcañices area (Fig. 3). Both levels are interbedded in the lowermost part of the Paraño Group, beneath the quartzite and the volcanic layers located more to the NW, in the Verín Synform, and dated as c. 439Ma by Valverde-Vaquero *et al.* (2007). They are lenticular bodies of felsic metavolcanites with variable thickness (up to 150m) and some kilometers in lateral extent.

COS-7: Located in the village of Soutelo (Portugal, 41° 53' 18.39"N / 6° 48' 23.71"W), it is a rhyolitic to rhyodacitic crystal-rich tuffaceous sandstone (nomenclature based on McPhie *et al.*, 1993), with porphyritic features and a crystal content up to 70%. The rock is constituted by

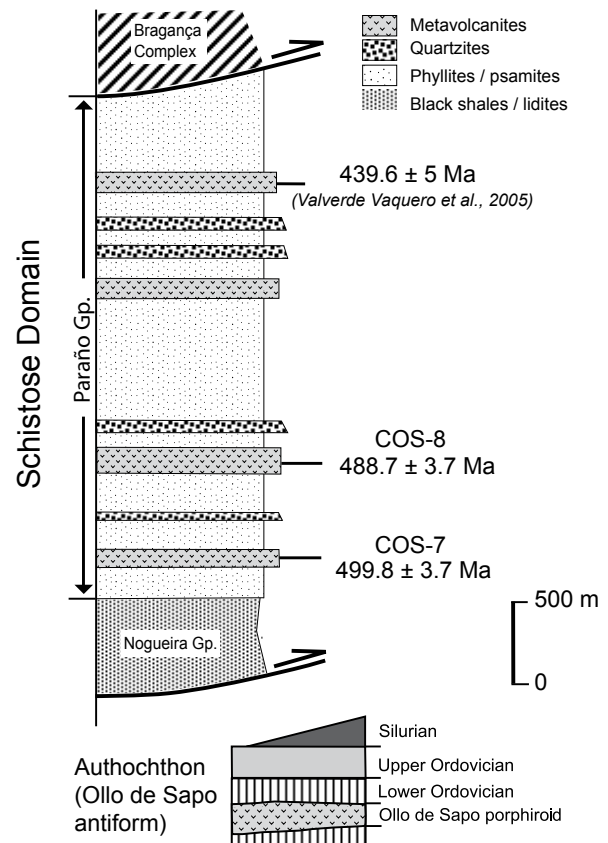


FIGURE 2. Synthetic stratigraphic column of the Schistose Domain in the NE limb of the Verín-Bragança Synform, showing the stratigraphic location of the collected samples and the samples dated by Valverde-Vaquero *et al.* (2007).

quartz (up to 3,5mm in size and an abundance of 30–35%), K-feldspar (Kfs, up to 3mm in size and an abundance of 15%), plagioclase (Pl, 5%) and biotite (3%), with minor sedimentary clasts (slates and fine to very fine grained sandstone) and vitreous clasts (totally replaced by sericite + hematite), in a very fine grained matrix composed by sericite and quartz that obliterates any previous vitreous texture of the matrix (Fig. 4A). All components are slightly rounded. Neither internal orientation of crystals nor grain classification can be observed (Fig. 4D). The rock is affected by a hydrothermal and/or metamorphic event, with development of a sericitic alteration. Pl and Kfs are partially replaced by sericite + quartz, and biotite is replaced by prehnite, sericite, hematite and titanite (Fig. 4E).

COS-8: Located in the road from Villarino de Manzanas to Figueruela (Spain, 41° 53' 15.20"N / 6° 28' 59.77"W), it is a porphyritic dacitic crystal-rich tuffaceous sandstone (55% of crystals), with an unevenly internal strain with development of deformation planes of 1–4mm in size. The rock is crosscut by millimetrically spaced quartz veins of 0.2–1mm width and millimetric to centimetric length (Fig. 4C). This rock is made up of idiomorphic to subidiomorphic crystals of K-feldspar (25%) 2mm in size as well as quartz

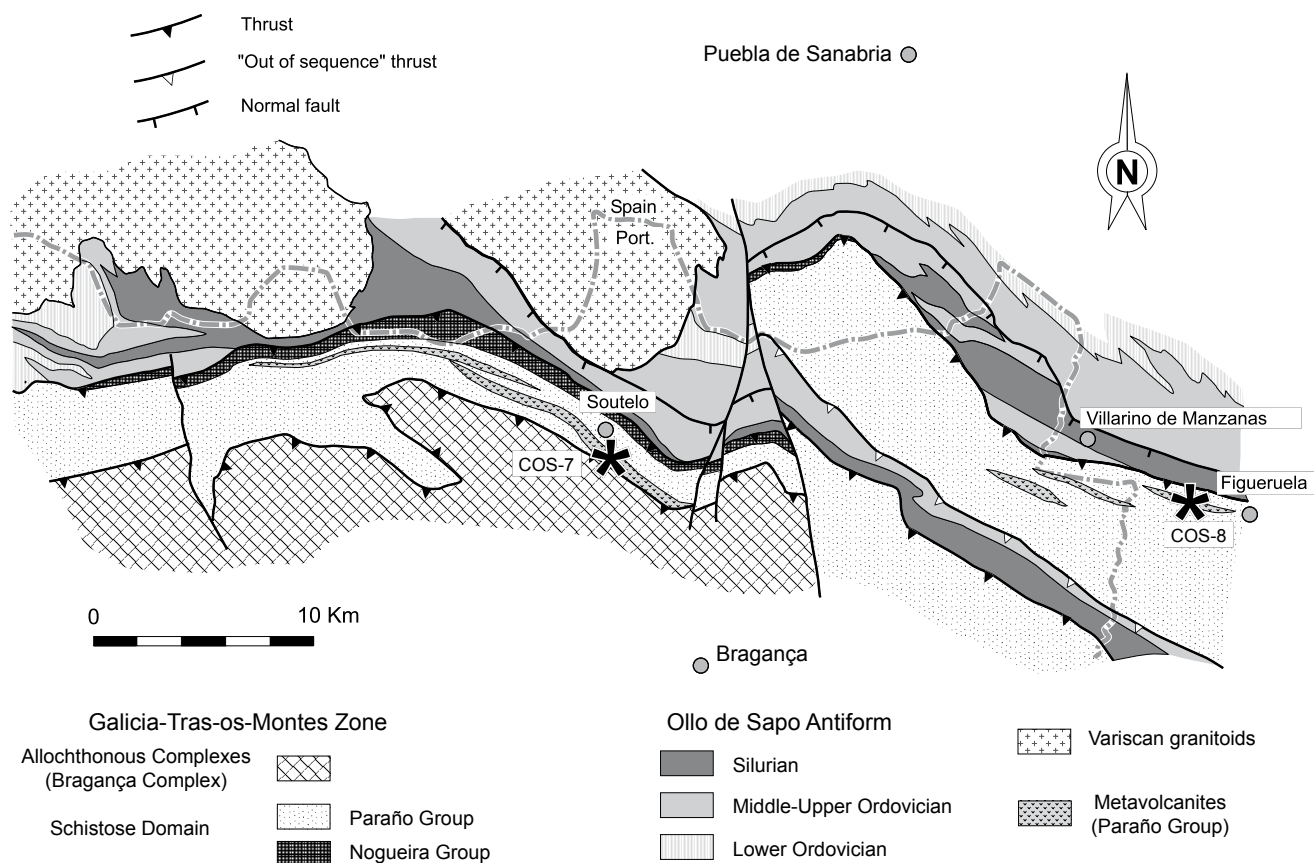


FIGURE 3. Geological map of the area located between Puebla Sanabria and Bragança (see Fig. 1) along the Spanish–Portuguese border, showing the location of the collected samples.

(18–20%) with sizes up to 3mm. Crystal fragments of both minerals with allotriomorphic forms are present (Fig. 4F). Plagioclase (5%) and biotite (3%) are also present. A pervasive sericitic alteration can be easily recognized in this sample. Biotite is totally replaced by sericite, hematite and titanite and K-feldspar is replaced by sericite. The matrix consists of a very fine grained granoblastic mass of quartz + sericite + caolinite, but previous spherulitic and perlitic vitreous textures can be observed (Fig. 4G).

ANALYTICAL TECHNIQUES

Zircons for isotope analyses were separated, after crushing and sieving, using an electromagnetic drum separator, heavy liquids as well as a Frantz isodynamic separator. The zircons were subsequently studied using a scanning electron microscope (SEM) equipped with secondary-electron and cathodoluminescence (CL) detectors at the Australian National University (ANU), Canberra, Australia.

The isotopic analysis of these domains was made at the Research School of Earth Sciences (RSES) of the ANU, by

means of a SHRIMP-II providing determinations of age based on isotopic analysis of U–Th–Pb in the CL-identified. For a full description of the ion-microprobe technique and data acquisition see Compston *et al.* (1984, 1986).

The U–Pb data are presented in Table 1 (errors are given as 1σ , the individual ages were calculated from the radiogenic $^{206}\text{Pb}/^{238}\text{U}$ and plotted into Tera–Wasserburg diagram (Tera and Wasserburg, 1972). Error boxes and single spot ages are 1σ . Average $^{206}\text{Pb}/^{238}\text{U}$ ages are given as weighted means (WM) and errors are expressed at the 95% confidence level, unless otherwise stated. ‘n’ are numbers of spots analysed / number of zircon crystals.

RESULTS

Soutelo rhyolite (Sample COS-7)

The examined zircons are transparent, mainly elongated and vary from euhedral or subhedral to rounded. In terms of CL-images, the occurrence of inherited cores prevails (95% of the zircons examined contain cores).

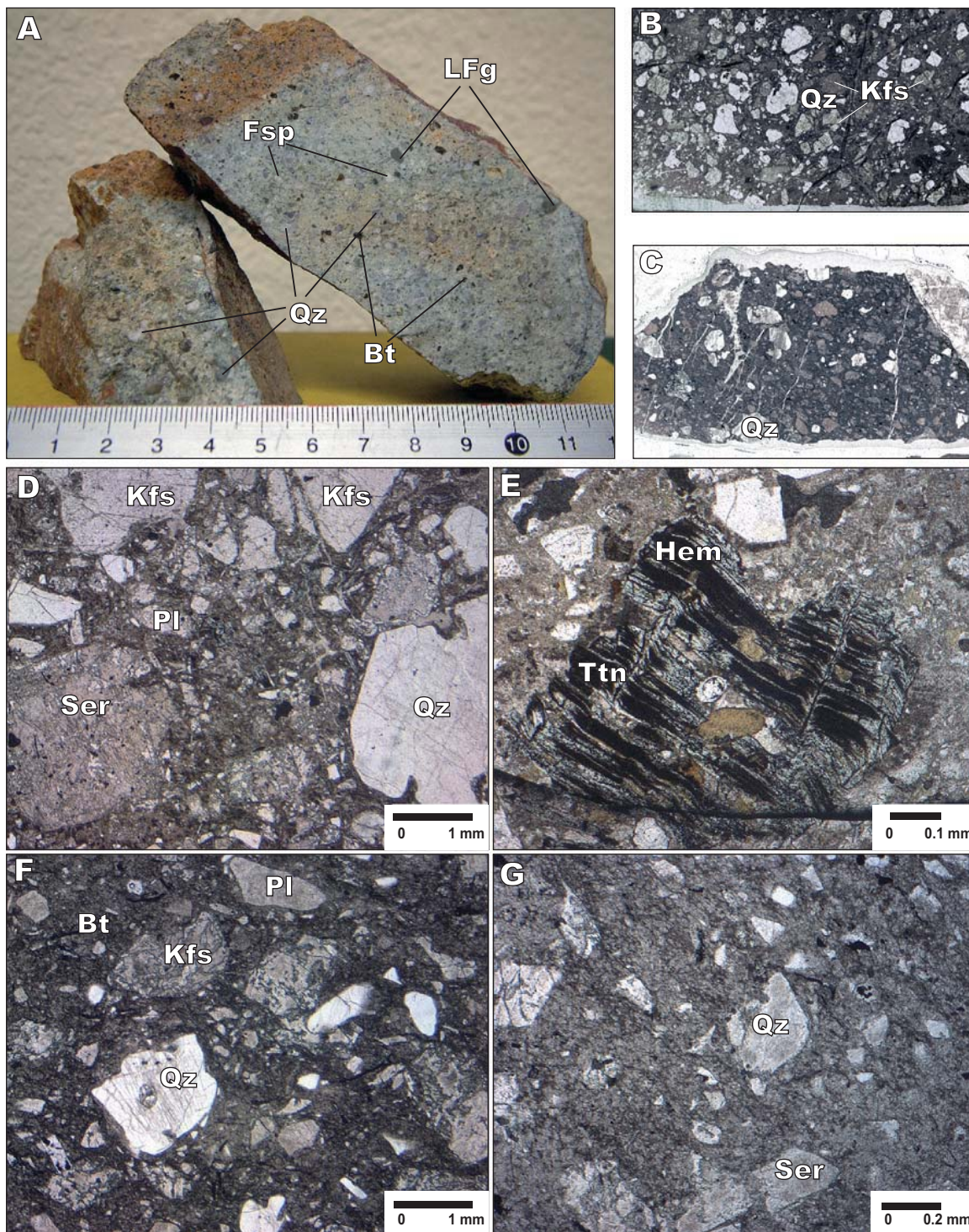


FIGURE 4. Several features of the analyzed samples. Main phases are pinpointed (abbreviation names of mineral based on Whitney and Evans, 2010, except LFg: lithic fragment). A) Macroscopic photograph of COS-07 sample. An orange weathering rim can be observed, but no sorting or orientation can be detected in rock fragment. B) Photomicrograph of COS-07 sample (base of image are 4 cm length). The abundance of main phases can be observed (Qz and Kfs) and the typical volcanic features of quartz. C) Photomicrograph of COS-08 sample (base of image are 4cm length). It is possible to observe the presence of quartz veins with the same orientation and an irregular distribution. A slightly orientation of rock can be deduced based on main mineral phases. D) Microscopical feature of COS-07 sample with polarized light. Alteration of feldspars and porphydic features can be observed as well as the edges slightly rounded of quartz crystals. E) Detailed aspect of a totally altered biotite in COS-07 sample. Biotite is replaced by prehnite + sericite (with colour into the exfoliation planes), hematite (Hem) and titanite (Ttn) (leucoxene). F) Microscopical aspect of COS-08 sample under cross polarized light. As in COS-07, quartz and plagioclase can be observed, with typical features of volcanic crystals and slightly rounded in their edges. G) Detailed aspect of another zone of COS-08 sample with a recrystallized vitreous matrix that preserves a previous spherulitic and perlitic hydration textures.

TABLE 1. Ion-microprobe data of single zircons from the Soutelo rhyolite (COS-7) and Alcañices dacite (COS-8). Pb* = Radiogenic Pb. Error in FC1 reference zircon calibration was 0.76% for the analytical session. ^{206}Pb % denotes the percentage of ^{206}Pb that is common Pb. Correction for common Pb for the U/Pb data has been made using the measured $^{238}\text{U}/^{206}\text{Pb}$ and $^{207}\text{Pb}/^{206}\text{Pb}$ ratios, following Tera and Wasserburg (1972) as outlined in Williams (1998). Standard deviation (1σ). * Denote outliers from the mean age

Grain.	U	Th	Th/U	$^{206}\text{Pb}^*$	$^{204}\text{Pb}/^{206}\text{Pb}$	f_{206}	Total				Radiogenic		Age (Ma)		CL pattern
							$^{238}\text{U}/^{206}\text{Pb}$	$^{207}\text{Pb}/^{206}\text{Pb}$	$^{206}\text{Pb}/^{238}\text{U}$	$^{206}\text{Pb}/^{207}\text{Pb}$	^{238}U	^{206}Pb	^{238}U	^{206}Pb	
spot	(ppm)	(ppm)		(ppm)		%	\pm	\pm	\pm	\pm	\pm	\pm	\pm		
COS-7 Soutelo volcanics															
<u>Inherited</u>															
4.1*	579	301	0,52	49,8	0,000024	<0,01	9,987	0,110	0,0592	0,0005	0,1003	0,0011	616,01	6,64	planar oscillatory
6.1*	470	45	0,09	133,4	0,000025	3,29	3,028	0,034	0,1379	0,0011	0,3194	0,0043	1786,74	20,92	planar oscillatory core
8.1*	711	50	0,07	50,7	-	0,02	12,043	0,132	0,0577	0,0006	0,0830	0,0009	514,13	5,50	weak zoning
15.1*	193	112	0,58	14,3	0,000112	<0,01	11,623	0,192	0,0560	0,0009	0,0863	0,0015	533,34	8,62	planar oscillatory
16.1*	477	33	0,07	34,2	0,000111	<0,01	11,976	0,183	0,0574	0,0008	0,0835	0,0013	517,13	7,71	weak zoning
<u>Protolith</u>															
1,1	713	149	0,21	49,4	0,000038	0,07	12,396	0,138	0,0578	0,0005	0,0806	0,0009	499,80	5,44	planar oscillatory rim
3,1	278	29	0,10	19,3	0,000052	<0,01	12,400	0,160	0,0546	0,0028	0,0809	0,0011	501,58	6,56	planar oscillatory rim
5,1	486	53	0,11	33,0	0,000102	0,03	12,651	0,246	0,0572	0,0006	0,0790	0,0016	490,29	9,31	rim weak zoning
7,1	252	49	0,19	17,3	-	<0,01	12,515	0,201	0,0556	0,0008	0,0801	0,0013	496,46	7,81	planar oscillatory rim
9,1	292	43	0,15	19,9	0,000050	<0,01	12,597	0,153	0,0562	0,0008	0,0795	0,0010	492,89	5,87	planar oscillatory rim
10,1	497	24	0,05	34,6	0,000059	<0,01	12,341	0,244	0,0564	0,0006	0,0811	0,0016	502,80	9,73	planar oscillatory rim
6,2	566	59	0,10	39,2	0,000045	0,07	12,407	0,230	0,0578	0,0005	0,0805	0,0015	499,38	9,05	planar oscillatory rim
11,1	408	47	0,12	28,7	-	<0,01	12,195	0,207	0,0561	0,0007	0,0821	0,0014	508,85	8,43	planar oscillatory rim
12,1	596	27	0,05	42,1	0,000071	<0,01	12,168	0,155	0,0574	0,0005	0,0822	0,0011	509,20	6,36	rim weak zoning
13,1	419	53	0,13	29,0	-	<0,01	12,423	0,152	0,0565	0,0007	0,0806	0,0010	499,52	5,99	planar oscillatory rim
14,1	377	61	0,16	25,9	0,000047	0,08	12,543	0,149	0,0577	0,0007	0,0797	0,0010	494,13	5,74	planar oscillatory rim
17,1	427	42	0,10	29,7	0,000088	<0,01	12,340	0,140	0,0553	0,0007	0,0812	0,0009	503,51	5,59	planar oscillatory rim
<u>Pb loss</u>															
2.1*	441	117	0,27	28,8	0,000036	0,18	13,169	0,188	0,0579	0,0007	0,0758	0,0011	471,01	6,60	planar oscillatory
COS-8 Alcañices volcanics															
<u>Inherited</u>															
3.1*	345	110	0,32	24,6	0,000432	0,53	12,046	0,138	0,0618	0,0009	0,0826	0,0010	511,48	5,77	planar oscillatory
3.2*	170	75	0,44	11,9	-	<0,01	12,316	0,157	0,0569	0,0011	0,0812	0,0011	503,53	6,31	planar oscillatory core
16.1*	353	177	0,50	105,8	0,000019	0,53	2,867	0,040	0,1223	0,0006	0,3470	0,0056	1920,21	26,84	planar oscillatory
<u>Protolith</u>															
1,1	304	55	0,18	20,2	-	0,26	12,887	0,152	0,0588	0,0008	0,0774	0,0009	480,56	5,55	planar oscillatory
2,1	325	62	0,19	22,5	-	<0,01	12,405	0,176	0,0564	0,0008	0,0807	0,0012	500,26	6,94	planar oscillatory rim
4,1	422	36	0,09	28,7	-	0,10	12,652	0,146	0,0578	0,0007	0,0790	0,0009	489,88	5,55	planar oscillatory
5,1	809	50	0,06	53,9	0,000025	<0,01	12,888	0,143	0,0567	0,0005	0,0776	0,0009	481,74	5,24	rim weak zoning
6,1	407	36	0,09	27,3	0,000115	<0,01	12,823	0,204	0,0566	0,0009	0,0780	0,0013	484,19	7,56	planar oscillatory
7,1	508	41	0,08	34,3	0,000072	<0,01	12,721	0,147	0,0561	0,0009	0,0787	0,0009	488,27	5,56	planar oscillatory rim
8,1	543	65	0,12	37,5	0,000063	<0,01	12,447	0,140	0,0567	0,0009	0,0804	0,0009	498,42	5,48	planar oscillatory rim
9,1	768	36	0,05	52,3	0,000049	<0,01	12,627	0,143	0,0559	0,0005	0,0793	0,0009	491,96	5,45	planar oscillatory rim
10,1	409	30	0,07	27,4	0,000051	0,07	12,820	0,180	0,0573	0,0007	0,0780	0,0011	483,88	6,64	planar oscillatory rim
12,1	661	45	0,07	45,2	-	<0,01	12,554	0,141	0,0568	0,0006	0,0797	0,0009	494,22	5,43	planar oscillatory rim
13,1	381	30	0,08	25,6	0,000174	-0,03	12,783	0,184	0,0566	0,0008	0,0783	0,0011	485,69	6,85	planar oscillatory rim
14,1	665	55	0,08	44,9	-	<0,01	12,706	0,142	0,0569	0,0006	0,0787	0,0009	488,42	5,33	rim weak zoning
15,1	599	58	0,10	40,4	0,000004	0,20	12,741	0,145	0,0585	0,0006	0,0783	0,0009	486,17	5,42	planar oscillatory rim
<u>Pb loss</u>															
11.1*	321	128	0,40	21,1	0,000111	0,32	13,039	0,154	0,0592	0,0009	0,0764	0,0009	474,85	5,53	planar oscillatory
17.1*	474	40	0,08	27,5	-	0,39	14,796	0,171	0,0583	0,0008	0,0673	0,0008	420,00	4,78	planar oscillatory rim

They are often rounded with planar oscillatory pattern and, sometimes, resorbed areas. Surrounding the cores, there is new crystallization of euhedral rims with either oscillatory pattern (*e.g.* zircons 11 and 7; Fig. 5). The described rims evidence overgrowth during a magmatic stage. In terms of SHRIMP-analyses the inner cores reveal the presence of distinct provenance ages (although this was not the purpose of this work).

Data are shown in Table 1 and the TW-diagrams in Figure 5. An inherited zircon yielded a $^{206}\text{Pb}/^{238}\text{U}$ age of 1.8Ga. Inherited components due to mixing of cores and rim in the analysis is evidenced by spots 15.1, 16.1 and 8.1. Zircon 2.1 shows some partial Pb loss. The rest of the data define a quasi-Gaussian distribution yielding an average age of $499.8 \pm 3.7\text{Ma}$ obtained on 12 spots located in rims within 12 crystals. The zircon domains analysed have U contents of 252 to 713ppm, and Th contents of 24 to 149ppm and the Th/U ratios range from 0.05 to 0.21. This age is interpreted as the age of the protolith formation.

Alcañices dacite (Sample COS-8)

Zircons are idiomorphic, euhedral with elongated tips. The CL-images show inner cores, often rounded (*e.g.* zircon 7; Fig. 6) with an oscillatory pattern surrounded by planar oscillatory domains, that show elongated tips with oscillatory pattern (*e.g.* zircons 7 and 13; Fig. 6). The CL-patterns allow us to assume a magmatic character of the zircons. They are euhedral elongated tips, planar oscillatory domains. Cores were rounded and sometimes resorbed before new crystallization occurred. Cores are very frequent (74% of the zircons examined contain cores).

Data are shown in Table 1 and the TW-diagram in Figure 6. It shows a $^{206}\text{Pb}/^{238}\text{U}$ age of 1.9Ga for an inherited zircon (spot 16.1) and the presence of Pb-loss (spot 11.1, 17.1). The rest of the data define a quasi-Gaussian distribution yielding an average age of $488.7 \pm 3.7\text{Ma}$ obtained on 13 spots located in rims within 13 crystals. This age is interpreted as the age of the protolith formation. Inherited

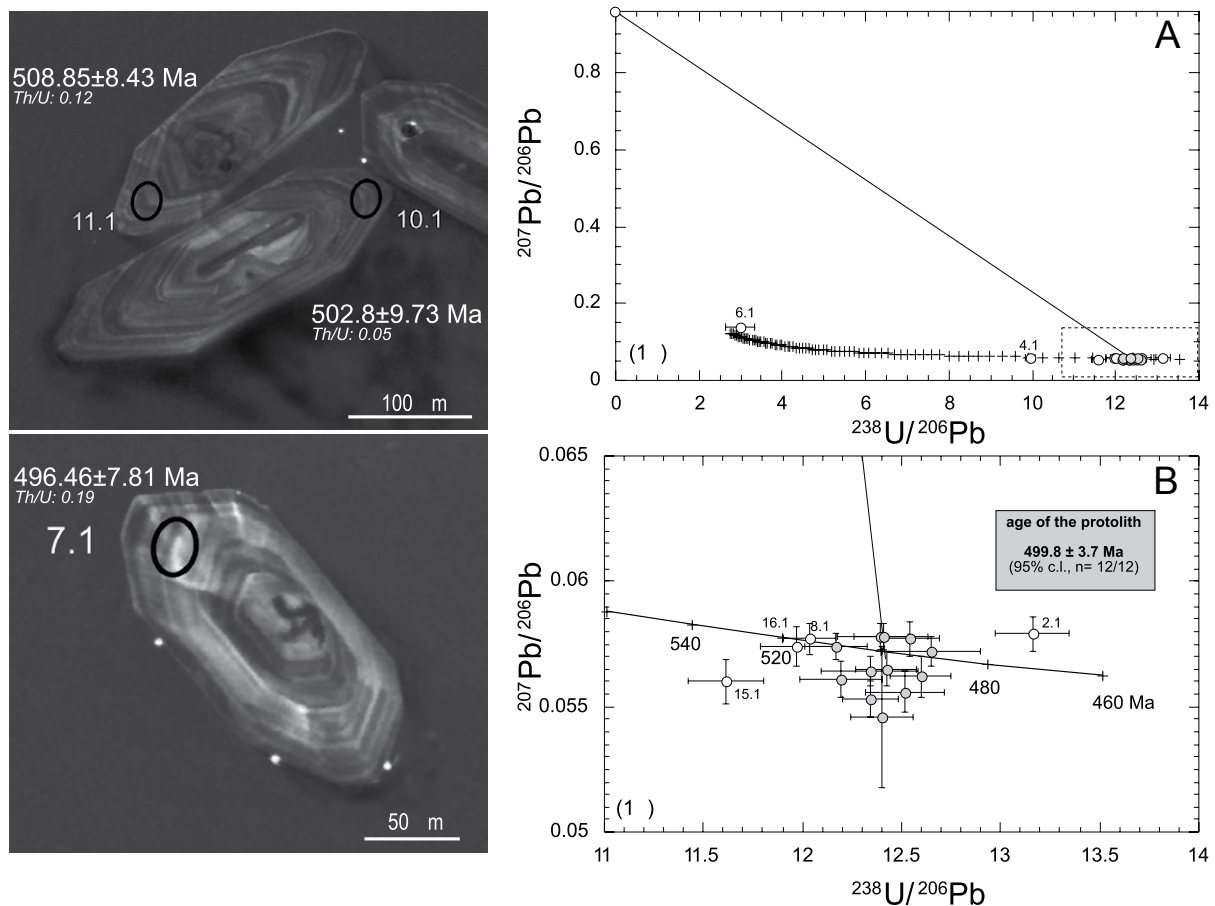


FIGURE 5. Cathodoluminescence images of zircons from the Soutelo rhyolite (COS-7). Zircons: n° 7.1, 10.1 and 11.1. A) U-Pb Tera-Wasserburg diagram for zircons from the Soutelo rhyolite (COS-7) showing all the data points; B) Enlargement of A. Error boxes are plotted as 1. Average $^{206}\text{Pb}/^{238}\text{U}$ ages are given as weighted means and errors are expressed at the 95% confidence level. The small numbers denote the spot number. Filled symbols in the TW-diagrams show the population that lie on the mixing lines. 'n' denotes 12 spots on 12 zircon crystals for the protolith population.

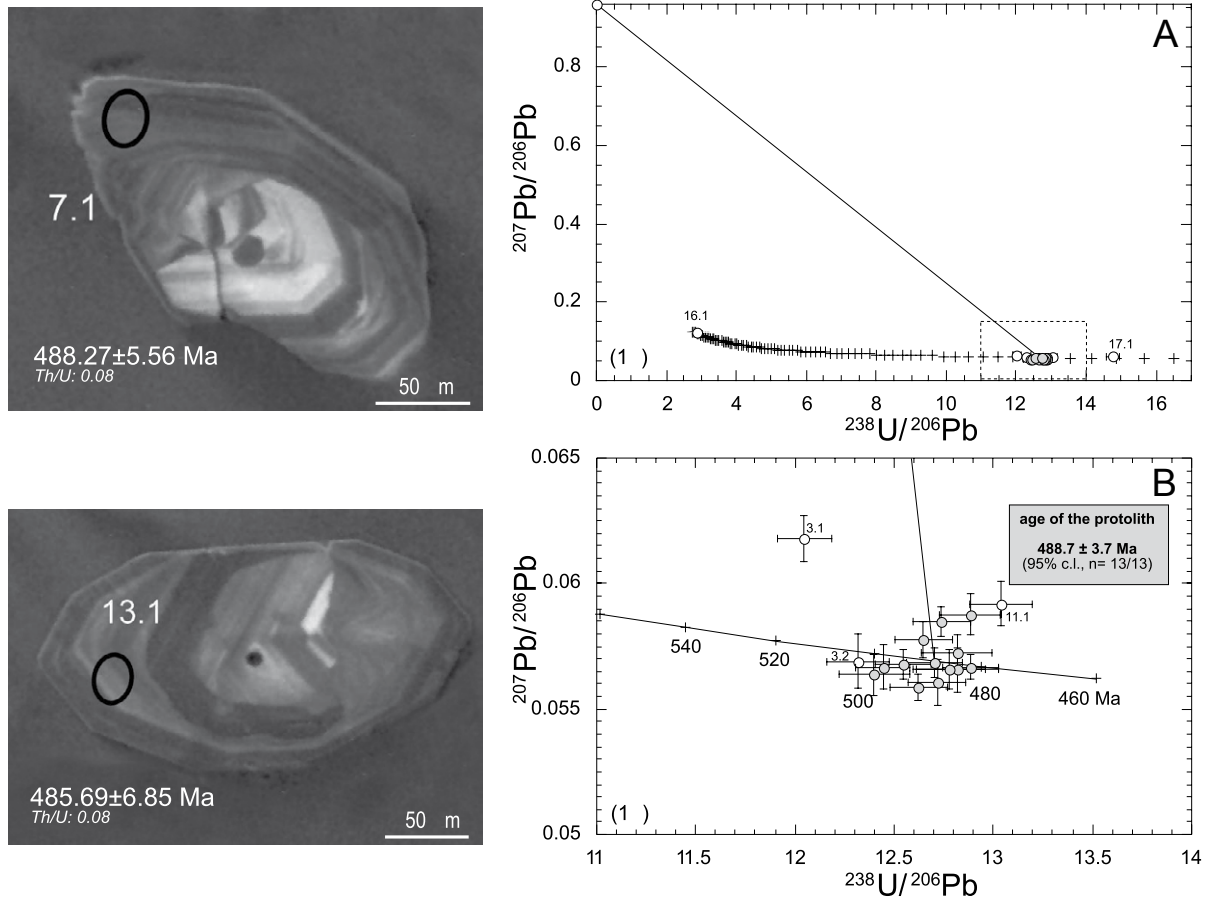


FIGURE 6. Cathodoluminescence images of zircons from the Alcañices dacite (COS-8). Zircons: n° 7.1 and 13.1. A) U–Pb Tera-Wasserburg diagram for zircons from the Alcañices dacite (COS-8) showing all the data points; B) Enlargement of A. Error boxes are plotted as 1 . Average $^{206}\text{Pb}/^{238}\text{U}$ ages are given as weighted means and errors are expressed at the 95% confidence level. The small numbers denote the spot number. Filled symbols in the TW-diagrams show the population that lie on the mixing lines. ‘n’ denotes 13 spots on 13 zircon crystals for the magmatic population.

component due to mixing of cores and rim in the analysis is evidenced by spots 3.1 and 3.2. The domains that define the main cluster have U contents of 304–809ppm, Th contents of 30–65ppm and Th/U ratios that vary from 0.05 to 0.19.

DISCUSSION AND CONCLUSIONS

The Schistose Domain of the Galicia-Trás-os-Montes Zone has been interpreted as the outboard edge of the Iberian terrane. The Soutelo rhyolite and the Alcañices dacite correspond to the lowermost levels of the Paraño Group in the northeast limb of the Verín-Bragança synform and according to the data presented we can propose a protolith age around $499.8 \pm 3.7\text{Ma}$ (Upper Cambrian) and $488.7 \pm 3.7\text{Ma}$ (Upper Cambrian–Lower Ordovician), respectively. These ages are older than the ones obtained by U–Pb zircon conventional techniques of $439.6 \pm 5\text{Ma}$ (Silurian) for a felsic trachyte in the middle part of the Paraño Group in the Verin Synform (Valverde-Vaquero *et al.*, 2007), and an age of $475 \pm 2\text{Ma}$ (Lower Ordovician) for a rhyolite

in equivalent series near Cabo Ortegal (Valverde-Vaquero *et al.*, 2005). According to the overall data, the age of the Paraño Group ranges from the uppermost Cambrian to, at least, lower Silurian.

Series of lower–Middle Ordovician felsic magmatism described in the autochthon of the Schistose Domain, the Olló de Sapo Antiform of the CIZ (Valverde-Vaquero and Dunning, 2000), include the Olló de Sapo Formation (Fm.), formed by hundreds of meters of metavolcanic, volcanosedimentary and igneous rocks with similar chemical signature to the acidic volcanites of the Paraño Group (Gallastegui *et al.*, 1987; Montero *et al.*, 2009). Apart from their siliciclastic and volcanic character, the Lower Paleozoic formations of the Olló de Sapo Domain (CIZ) and the Paraño Group (GTMSD) are quite different. Nonetheless, the presence of few Pan-African detrital zircons within the Alcañices and Soutelo volcanics with ages around 600–500Ma indicates their derivation from Gondwana. Moreover, both include inherited zircons with provenance ages of ca. 1.8Ga. Similar ages have been

reported in other zones of the Iberian Massif (i.e. Cabo Ortegal Complex, Ordóñez-Casado *et al.*, 2001, Ossa Morena Zone, Ordóñez-Casado, 1999 and West Asturian Leonese Zone, Fernández-Suárez *et al.*, 2013 and Rubio-Ordóñez *et al.*, in press). This is consistent with the interpretation made in several previous works, locating the Galicia Trás os Montes Schistose Domain in the most external part of the continental margin of Gondwana (Farias *et al.*, 1987; Gallastegui *et al.*, 1987; Ribeiro *et al.*, 1990; Martínez Catalán *et al.*, 1999; Marcos *et al.*, 2002; Murphy *et al.*, 2008; Díez Fernández *et al.*, 2012).

ACKNOWLEDGMENTS

This research was supported by research projects MEC CGL2006-08822, MICINN CGL2010-14890 and CONSO-LIDER-INGENIO CE-CSD2006-00041. We acknowledge J. Fernández-Suárez and an anonymous reviewer for their constructive comments and corrections.

REFERENCES

- Arenas, R., Martínez Catalán, J.R., Díaz García, F., 2004a. Complejos alóctonos de Galicia-Trás-os-Montes. In: Vera, J.A. (ed.). Geología de España. Madrid, Sociedad Geológica de España-Instituto Geológico y Minero de España (SGE-IGME), 138-162.
- Arenas, R., Martínez Catalán, J.R., Díaz García, F., 2004b. Zona de Galicia-Trás-os-Montes: introducción. In: Vera, J.A. (ed.). Geología de España. Madrid, Sociedad Geológica de España-Instituto Geológico y Minero de España (SGE-IGME), 133-135.
- Barrera, J.L., Farias, P., González Lodeiro, F., Marquínez, J.L., Martín Parra, L.M., Martínez Catalán, J.R., Olmo Sanz, A. del, Pablo Maciá, J.G. de, 1989. Mapa y memoria de la Hoja nº 17-27 (Orense-Verín) del Mapa Geológico de España, Escala 1/200.000. Madrid, Instituto. Geológico y Minero de España.
- Bastida, F., Marcos, A., Marquínez, J., Martínez Catalán, J.R., Pérez-Estaún, A., Pulgar, J.A., 1984. Mapa Geológico de España, Hoja nº 1 (2-1) (La Coruña) y memoria explicativa Escala. 1/200.000. Madrid, Instituto. Geológico y Minero de España, 155pp.
- Compston, W., Kinny, P.D., Williams, I.S., Foster, J.J., 1986. The age and Pb loss behaviour of zircons from the Isua supracrustal belt as determined by ion microprobe. *Earth Planetary Science Letters*, 80, 71-81.
- Compston, W., Williams, I.S., Meyer, C., 1984. U-Pb geochronology of zircons from lunar breccia 73217 using a sensitive high mass-resolution ion microprobe. *Journal of Geophysical Research*, B89, 525-534.
- Dallmeyer, R.D., Martínez Catalán, J.R., Arenas, R., Gil Ibarra, J.I., Gutiérrez Alonso, G., Farias, P., Aller, J., Bastida, F., 1997. Diachronous Variscan tectonothermal activity in the NW Iberian Massif: Evidence from $^{40}\text{Ar}/^{39}\text{Ar}$ dating of regional fabrics. *Tectonophysics*, 277, 307-337.
- Díez Fernández, R., Martínez Catalán, J.R., Arenas, R., Abati, J., Gerdes, A., Fernández-Suárez, J., 2012. U-Pb detrital zircon analysis of the lower allochthon of NW Iberia: age constraints, provenance and links with the Variscan mobile belt and Gondwanan cratons. *Journal of the Geological Society*, 169, 655-665.
- Farias, P., 1990. La geología de la Región del Sinforme de Verín (Cordillera Herciniana, NW de España). *Nova Terra*, 2, 1-201.
- Farias, P., Gallastegui, G., González Lodeiro, F., Marquínez, J., Martín-Parra, L.M., Martínez Catalán, J.R., Pablo Maciá, J.G. de, Rodríguez-Fernández, L.R., 1987. Aportaciones al conocimiento de la litoestratigrafía y estructura de Galicia Central. *Memoria Faculdade de Ciências da Universidade do Porto*, 1, 411-431.
- Ferragne, A., 1972. Le Précambrien et le Paléozoïque de la Province de l'Orense (Nord-Ouest de l'Espagne). *Stratigraphie-Tectonique-Métamorphisme*. Doctoral Thesis, Université de Bordeaux, 249pp.
- Fernández Pompa, F., Monteserín López, V., 1976. Mapa y memoria explicativa de la Hoja 7 (Cedeira) del Mapa Geológico de España. Escala 1/50.000. Madrid, Instituto. Geológico y Minero de España, 2ª Serie.
- Fernández-Suárez, J., Gutiérrez-Alonso, G., Pastor-Galán, D., Hofmann, M., Murphy, J. B., Linnemann, U., 2013. The Ediacaran-Early Cambrian Detrital Zircon Record of NW Iberia: Possible Sources and Paleogeographic Constraints. *International Journal of Earth Sciences*, 103(5), 1335-1357.
- Gallastegui, G., Martín Parra, L.M., Farias, P., Pablo Maciá, J.G. de, Rodríguez Fernández, L.R., 1987. Las metavulcanitas del Dominio Esquistoso de Galicia Trás-os-Montes: petrografía, geoquímica y ambiente geotectónico (Galicia, NO de España). *Cadernos do Laboratorio Xeolóxico de Laxe*, 12, 127-139.
- González Clavijo, E., 1997. La geología del Sinforme de Alcañices, oeste de Zamora. Doctoral Thesis. Salamanca, Universidad de Salamanca, 330pp.
- González Clavijo, E., Martínez Catalán, J.R., 2002. Stratigraphic record of preorogenic to synorogenic sedimentation, and tectonic evolution of imbricate units in the Alcañices synform (northwestern Iberian Massif). In: Martínez Catalán, J.R., Hatcher, R.D.Jr., Arenas, R., Díaz García, F. (eds.). *Variscan-Appalachian dynamics: The building of the late Paleozoic*. Geological Society of America, 364 (Special Paper), 17-35.
- Iglesias, M., Robardet, M., 1980. El Silúrico de Galicia Media-Central. Su importancia en la paleogeografía Varisca. *Cadernos do Laboratorio Xeolóxico de Laxe*, 1, 99-115.
- Julivert, M., Fontboté, J.M., Ribeiro, A., Nabais-Conde, L.E., 1972. Mapa tectónico de la Península Ibérica y Baleares a escala 1/1.000.000. Instituto Geológico y Minero de España, Memoria explicativa, 113pp.
- Lotze, F., 1945. Zur Gliederung der Varisziden der Iberischen Meseta. *Geotektonische Forschungen*, 6, 78-92. (Translated into Spanish in *Publicaciones Extranjeras Geología de España*, 5, 149-166).

- Marcos, A., Farias, P., 1999. La estructura de las láminas inferiores del Complejo de Cabo Ortegal y su autóctono relativo (Galicia, NO de España). *Trabajos de Geología*, 21, 201-221.
- Marcos, A., Farias, P., Galán, G., Fernández, J.J., Llana-Fúnez, S., 2002. Tectonic framework of the Cabo Ortegal Complex: A slab of lower crust exhumed in the Variscan orogen (northwestern Iberia Peninsula). In: Martínez Catalán, J.R., Hatcher, R.D.Jr., Arenas, R., Díaz García, F. (eds.). *Variscan-Appalachian dynamics: The building of the late Paleozoic basement*. Geological Society of America, 364 (Special Paper), 143-162.
- Marcos, A., Llana-Fúnez, S., 2002. Estratigrafía y estructura de la lámina tectónica del Para-autóctono y de su autóctono en el área de Chantada (Galicia, NO de España). *Trabajos de Geología*, 23, 53-72.
- Martínez Catalán, J.R., Arenas, R., Díaz García, F., Abati, J., 1999. Allochthonous units in the Variscan Belt of NW Iberia. In: Sinha, A.K. (ed.). *Terranes and Accretionary History, Basement Tectonics*. Netherlands, Kluwer Academic Publishers, 13, 65-84.
- Matte, P., 1968. La structure de la virgation hercynienne de Galice (Espagne). *Revue de Géologie Alpine*, 44, 1-128.
- McPhie, J., Doyle, M., Allen, R., 1993. *Volcanic textures: a guide to the interpretation of textures in volcanic rocks*. Hobart, Centre for Ore Deposit and Exploration Studies, University of Tasmania, 198pp.
- Montero, P., Talavera, C., Bea, F., Lodeiro, F.G., Whitehouse, M.J., 2009. Zircon Geochronology of the Ollo de Sapo Fm. and the age of the Cambro-Ordovician Rifting in Iberia. *The Journal of Geology*, 117, 174-191.
- Murphy, J.B., Gutiérrez Alonso, G., Fernández Suárez, J., Braid, J.A., 2008. Probing crustal and mantle lithosphere origin through Ordovician volcanic rocks along the Iberian passive margin of Gondwana. *Tectonophysics*, 461, 166-180.
- Ordóñez Casado, B., 1999. Geochronological studies of the Pre-Mesozoic basement of the Iberian Massif: the Ossa Morena zone and the Allochthonous Complexes within the Central Iberian zone. Doctoral Thesis. Zürich, Eidgenössische Technische Hochschule, 240pp.
- Ordóñez Casado, B., Gebauer, D., Schäfer, H.J., Gil Ibarguchi, J.I., Peucat, J.J., 2001. A single Devonian subduction event for the high-pressure/high-temperature ultramafic-mafic and country rocks of the Cabo Ortegal Complex (NW Spain). *Tectonophysics*, 332, 359-385.
- Pereira, E., Ribeiro, A., Marques, F., Munhá, J., Meireles, C., Ribeiro, M.A., Pereira, D., Noronha, F., Ferreira, N., 2000. Carta Geológica de Portugal, Escala 1/200.000. Lisboa. Serviço Geológico de Portugal. Folha 2.
- Piçarra, J.M., Gutiérrez Marco, J.C., Sá, A.A., Meireles, C., González Clavijo, E., 2006. Silurian graptolite biostratigraphy of the Galicia-Tras-os-Montes Zone (Spain and Portugal). *GFF*, 128, 185-188.
- Ribeiro, A., 1974. Contribution a l'étude tectonique de Trás-os-Montes Oriental. *Memória Serviço Geológico Portugal*, 24, 1-179.
- Ribeiro, A., Pereira, E., Dias, R., 1990. Structure in the NW of the Iberian península. In: Dallmeyer, R.D, Martínez-García, E. (eds.). *Pre-Mesozoic Geology of Iberia*. Berlín, Springer-Verlag, 221-236.
- Rodríguez, R., Marcos, A., Farias, P., 2004. Palynological data on the age of the metasediments of the Para-autochthonous thrust sheet in the Cabo Ortegal area (Galicia, NW Spain). *Neues Jahrbuch für Geologie und Geologie und Paläontologie*, 10, 437-447.
- Romariz, C., 1969. Graptolites silúricos do NW Peninsular. *Communication Serviço Geológico Portugal*, 53, 107-156.
- Rubio-Ordoñez, A., Gutierrez-Alonso, G., Valverde-Vaquero, P., Cuesta, A., Gallastegui, G., Gerdes, A., Cárdenes, V., in press. Arc-related Ediacaran magmatism along the northern margin of Gondwana: Geochronology and isotopic geochemistry from northern Iberia. *Gondwana Research*.
- Tera, F., Wasserburg, G., 1972. U-Th-Pb systematics in three Apollo 14 basalts and the problem of initial Pb in lunar rocks. *Earth Planetary Science Letters*, 14, 281-304.
- Valverde-Vaquero, P., Dunning, G.R., 2000. New U-Pb ages for Early Ordovician magmatism in Central Spain. *Journal of the Geological Society*, 157, 15-26.
- Valverde-Vaquero, P., Marcos, A., Farias, P., Gallastegui, G., 2005. U-Pb isotopic dating of the volcanic rocks of the Schistose Domain in the Cabo Ortegal area (Galicia, NW Spain): geodynamic consequences. *Geológica Acta*, 3(1), 27-37.
- Valverde-Vaquero, P., Farias, P., Marcos, A., Gallastegui, G., 2007. U-Pb dating of Siluro-Ordovician volcanism in the Verín Synform (Orense; Schistose Domain, Galicia-Trás-os-Montes Zone). *Geogaceta*, 41, 247-250.
- Whitney, D.L., Evans, B.W., 2010. Abbreviations for names of rock-forming minerals. *American Mineralogist*, 95, 185-187.
- Williams, I.S., 1998. U-Th-Pb Geochronology by Ion Microprobe. In: McKibben, M.A., Shanks III, W.C., Ridley, W.I. (eds). *Applications of microanalytical techniques to understanding mineralizing processes*, *Reviews in Economic Geology*, 7, 1-35

Manuscript received October 2013;

revision accepted June 2014;

published Online June 2014.